Distinct large-scale turbulent-laminar states in transitional pipe flow

David Moxey[1] and Dwight Barkley

Mathematics Institute, University of Warwick, Coventry, United Kingdom

Edited by Katepalli R. Sreenivasan, New York University, New York, and approved March 12, 2010 (received for review August 22, 2009)

When fluid flows through a channel, pipe, or duct, there are two basic forms of motion: smooth laminar motion and complex turbulent motion. The discontinuous transition between these states is a fundamental problem that has been studied for more than 100 yr. What has received far less attention is the large-scale nature of the turbulent flows near transition once they are established. We have carried out extensive numerical computations in pipes of variable lengths up to 125 diameters to investigate the nature of transitional turbulence in pipe flow. We show the existence of three fundamentally different turbulent states separated by two distinct Reynolds numbers. Below $Re_1 \simeq 2{,}300$, turbulence takes the form of familiar equilibrium (or longtime transient) puffs that are spatially localized and keep their size independent of pipe length. At Re_1 the flow makes a striking transition to a spatio-temporally intermittent flow that fills the pipe. Irregular alternation of turbulent and laminar regions is inherent and does not result from random disturbances. The fraction of turbulence increases with Re until $Re_2 \simeq 2{,}600$ where there is a continuous transition to a state of uniform turbulence along the pipe. We relate these observations to directed percolation and argue that Re_1 marks the onset of infinite-lifetime turbulence.

intermittency | puff | turbulence | directed percolation | lifetime

The transition to turbulence in pipe flow has occupied researchers since the pioneering work of Reynolds 125 years ago (1). Over the past decade the field has been very active on several fronts as reviewed in the collection of papers appearing in ref. 2. One may briefly summarize recent work as focusing on the dependence of transition thresholds with Reynolds number and the associated boundary or edge states between laminar and turbulent dynamics (3–6); unstable periodic traveling waves thought to offer keys to the structure and behavior of turbulent states near transition (7, 8); and lifetime measurements of turbulent puffs (9–11).

A separate line of research has emerged concerning alternating turbulent-laminar flow states on long length scales in subcritical shear flows (12–17). It has been established that in plane Couette flow (12–15), counterrotating Taylor-Couette flow (12, 13), and plane Poiseuille flow (16), near transition the system can exhibit a remarkable phenomenon in which turbulent and laminar flow form persistent alternating patterns on scales very long relative to wall separation and the spacing between turbulent streaks. While the origin of these patterns remains a mystery, they are intimately connected with the lower limit of turbulence in shear flows.

With these large-scale structures comes the view, shared by others (17), that system size can be a significant factor in shear flows near the lower Reynolds number limit of turbulence and that one needs to consider the spatio-temporal aspects of the flow on sufficiently long scales to correctly capture and understand the subcritical transition process. We shall show that this is indeed the case for pipe flow.

The goal of our study is, therefore, to quantify through extensive numerical simulations the fundamental aspects of large-scale turbulent-laminar states in pipe flow at transitional Reynolds numbers. For this we use axially periodic pipes of length L and diameter D, where L is both large and is varied as part of the study.

The flow is governed by the incompressible Navier-Stokes equations

$$\partial_t \mathbf{u} + (\mathbf{u}\cdot\nabla)\mathbf{u} = -\nabla p + \mathrm{Re}^{-1}\nabla^2\mathbf{u}, \quad \nabla\cdot\mathbf{u} = \mathbf{0} \qquad [1]$$

subject to periodic boundary conditions in the streamwise direction and no-slip conditions at the pipe walls. Lengths are nondimensionalized by D and velocities by the average streamwise velocity (bulk velocity) $\bar{U}$. Re is the Reynolds number. Without loss of generality the fluid density is fixed at one. We work in Cartesian coordinates $\mathbf{x} = (x, y, z)$, where x is aligned with the streamwise direction and the transverse coordinates (y, z) are centered on the pipe axis. The corresponding velocities are denoted by $\mathbf{u}(\mathbf{x}, t) = (u(\mathbf{x}, t), v(\mathbf{x}, t), w(\mathbf{x}, t))$, so that u is the axial and v and w are the transverse velocity components.

We perform direct numerical simulations using the mixed spectral-element-Fourier code *Semtex* (18). A spectral-element mesh similar to that presented in ref. 19 is used to represent y–z circular cross-sections, with elements concentrated near the pipe boundary to accurately resolve the boundary layer. A Fourier pseudospectral representation is used in the periodic axial direction. The flow is driven at constant volumetric flux using the Green's function method outlined in ref. 20, ensuring a constant, prescribed value of Re.

The simulations have been validated at $\mathrm{Re} = 5{,}000$ against well-established numerical data (19, 21), using an expansion basis of polynomial order 10, corresponding to 121 collocation points within each spectral element. Results presented here are at considerably lower Re and use the same polynomial order. This resolution is consistent with, and slightly finer than, that used in other validated simulations (22). We use between 512 (at $L = 8\pi$) and 2,048 (at $L = 40\pi$) Fourier modes (or grid points) in the axial direction. For simplicity we shall refer to $L = 8\pi = 25.132\ldots$ as $L = 25D$ and $L = 40\pi = 125.664\ldots$ as $L = 125D$, etc.

The computational protocol is of the reverse transition type (12, 23–26) where we always first obtain a fully turbulent flow throughout the pipe at $\mathrm{Re} \simeq 3{,}000$ and then decrease Re. Unlike other relaminarization studies (23, 24, 26), we do not decrease Re into the range where the flow fully relaminarizes. In this way we are able to move up and down the branch of turbulent solutions and explore their dependence on Re.

Results

Basic Phenomena. Fig. 1 summarizes the subject of our study. Results are presented from a long set of simulations in an $L = 125D$ pipe for Re from 2,800 decreasing to 2,250. The full output from all the simulations is condensed into a single space-time plot together with two flow visualizations—one at

Author contributions: D.M. performed research; and D.M. and D.B. wrote the paper.

The authors declare no conflict of interest.

This article is a PNAS Direct Submission.

[1]To whom correspondence should be addressed. E-mail: D.C.Moxey@warwick.ac.uk.

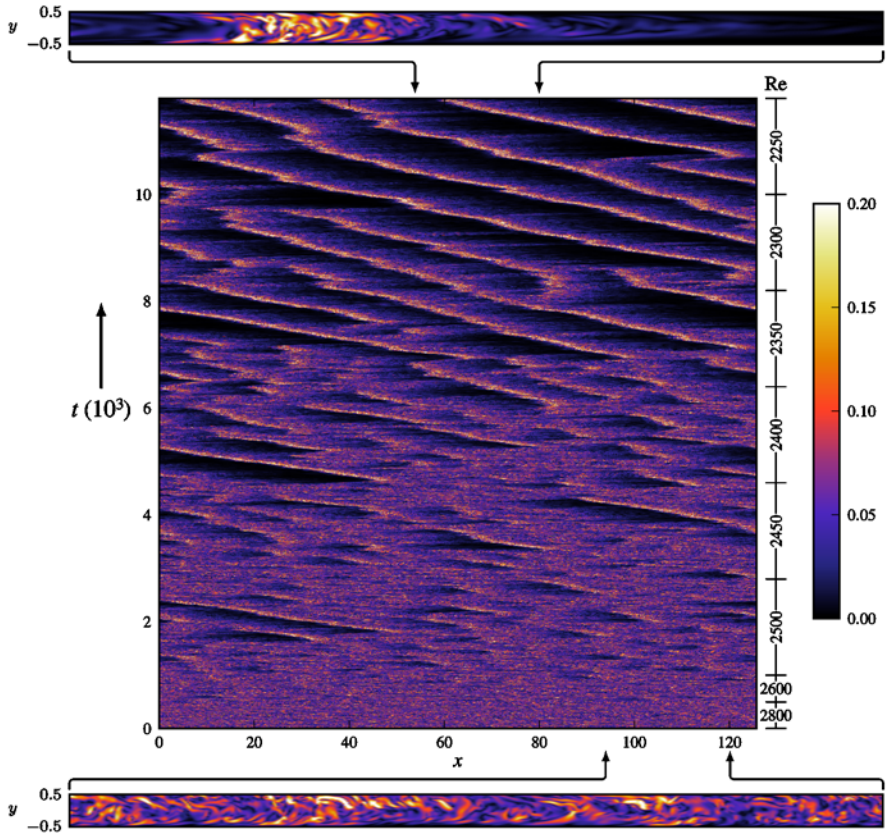

Fig. 1. Dynamics of transitional flow from simulations of a $L = 125D$ pipe. The central plot shows a space-time diagram with the streamwise direction horizontal and time increasing vertically upwards. The value of Re changes as indicated on the right. Plotted is the magnitude transverse velocity q sampled along the axis of the pipe and plotted in a frame moving at the average fluid velocity: $q(x - \bar{U}t, y = 0, z = 0, t)$. Colors are such that light corresponds to turbulent flow and black corresponds to laminar flow. Below and above are flow visualizations in vertical cross-sections through the pipe at the initial and final times, and over the $25D$ streamwise extents indicated by arrows.

the initial time and one at the final time. We have determined that the magnitude of transverse velocity provides the best single measure for visualizing and analyzing the features of interest. For compactness we denote this by q:

$$q = \sqrt{v^2 + w^2}. \qquad [2]$$

At each space-time point we plot $q(x - \bar{U}t, 0, 0, t)$; that is, the transverse velocity magnitude along the axis of the pipe, as seen in a frame moving at the average velocity. The relationship between one line of the space-time diagram and the instantaneous flow within the pipe is highlighted by the two flow visualizations showing a small representative portion, $25D$ in length, of the full pipe flow. Where the flow is turbulent, q fluctuates in space and time and is relatively large. Where the flow is laminar, q is nearly zero. For parabolic flow, $v = w = 0$, hence $q = 0$.

The initial condition for the simulation is a fully developed turbulent flow at $\mathrm{Re} = 2,800$. As time proceeds upwards, Re is decreased in discrete steps at the times indicated by ticks on the right of the figure. For example, $\mathrm{Re} = 2,800$ until $t = 500$ when it is changed to 2,600. The simulation then continues at this lower Re until the next change. At each Re, simulations are run sufficiently long that any transient effects disappear (very quickly on the timescale spanned by Fig. 1) and representative asymptotic dynamics at the corresponding Re are evident in the space-time diagram.

For $\mathrm{Re} \gtrsim 2,600$ the flow is turbulent throughout the length of the pipe. We call this uniform turbulence, referring to the fact that there is no large-scale variation in the turbulent structure along the pipe axis. This is to be contrasted with what is clearly seen at $\mathrm{Re} = 2,500$: regions of nearly laminar flow (dark) are seen to spontaneously appear and then disappear within the sea of turbulence. The flow is in an intermittent state. As Re decreases further, the proportion of laminar flow increases and the intermittent laminar flashes give rise to a more regular alternation of turbulent and laminar flow. The turbulent-laminar states are not, however, steady; there are some splitting and extinction events. Nevertheless, at the end of the simulation, there are four distinct turbulent regions separated by four regions of relatively laminar flow. The final visualization reveals that these are in fact four turbulent puffs of the type commonly observed in pipe flow at Re around 2,000 (3, 27–29).

Notice that since puffs move more slowly than the average velocity, the puffs are seen to propagate to the left in Fig. 1. In the "laboratory frame" in which the pipe is stationary, the flow is from left to right and puffs propagate quickly to the right.

Fig. 1 shows clearly the spontaneous emergence of turbulent puffs from uniform turbulence as Re is decreased from 2,800 to 2,250. The remainder of the paper will be devoted to analyzing in more detail the distinct states and transitions contained in Fig. 1. There are in fact two transitions over the range of Re considered. One, which is apparent in the figure, is the onset of intermittency at $\mathrm{Re}_2 \simeq 2,600$. The other is not obvious from Fig. 1 and occurs at $\mathrm{Re}_1 \simeq 2,300$. We shall address this latter transition first.

Transition Between Localized and Intermittent Turbulence. In Fig. 2 we demonstrate the radically different nature of the turbulent flows at $\mathrm{Re} = 2,250$ and $\mathrm{Re} = 2,350$ using an approach first taken in plane Couette flow (14). Fig. 2 *A* and *B* show space-time diagrams—again plotting q in the frame of the average velocity. On the left $\mathrm{Re} = 2,250$, while on the right $\mathrm{Re} = 2,350$. In both

cases the initial state is a single puff in an $L = 25D$ pipe. As time proceeds upwards L is increased in discrete steps of $5D$ until $L = 90D$. The difference in the resulting behavior in the two cases is visually striking. At $\mathrm{Re} = 2,250$ a single localized turbulent puff persists quite independently of L, whereas at $\mathrm{Re} = 2,350$ the number of puffs increases with pipe length so as to maintain approximately the same spatial scale of the turbulent-laminar alternation and therefore the same ratio of turbulent to laminar flow. The difference between the two states is further emphasized in Fig. 2 *C* and *D* showing velocity profiles at the final time of each simulation.

We focus first on $\mathrm{Re} = 2,250$. Once L is sufficiently large, the state is a localized equilibrium puff (3, 28) and its form is independent of further increases in L. Surrounding the turbulent puff is not merely laminar flow–far downstream, fully developed parabolic Hagen-Poiseuille flow is recovered, as in Fig. 2*C*, consistent with reversion through viscous dissipation (25). It is possible to observe or create multiple puffs in sufficiently long pipes at $\mathrm{Re} = 2,250$, as seen for example in Fig. 1, and of course all puffs computed in periodic pipes correspond to multiple puffs in longer pipes. Fundamentally, however, at $\mathrm{Re} = 2,250$ the long-time, large-domain state is persistent localized patches of turbulence, traveling at fixed (equilibrium) speed, residing in a background laminar flow. The turbulence can be viewed as an intensive quantity not dictated by domain size. It is determined by the number of puffs introduced into the flow, for example through initial conditions. For a fixed number of puffs, the domain size can be adiabatically increased and the total turbulent flow will remain constant.

This behavior holds for some range of Re below $\mathrm{Re} = 2,250$ until puffs cannot be sustained at all. This is the subject of study elsewhere (3, 4) and we have not explored it. As will be important in the discussion to follow, there is compelling evidence that all such localized puffs have a finite lifetime (9, 22, 30), although

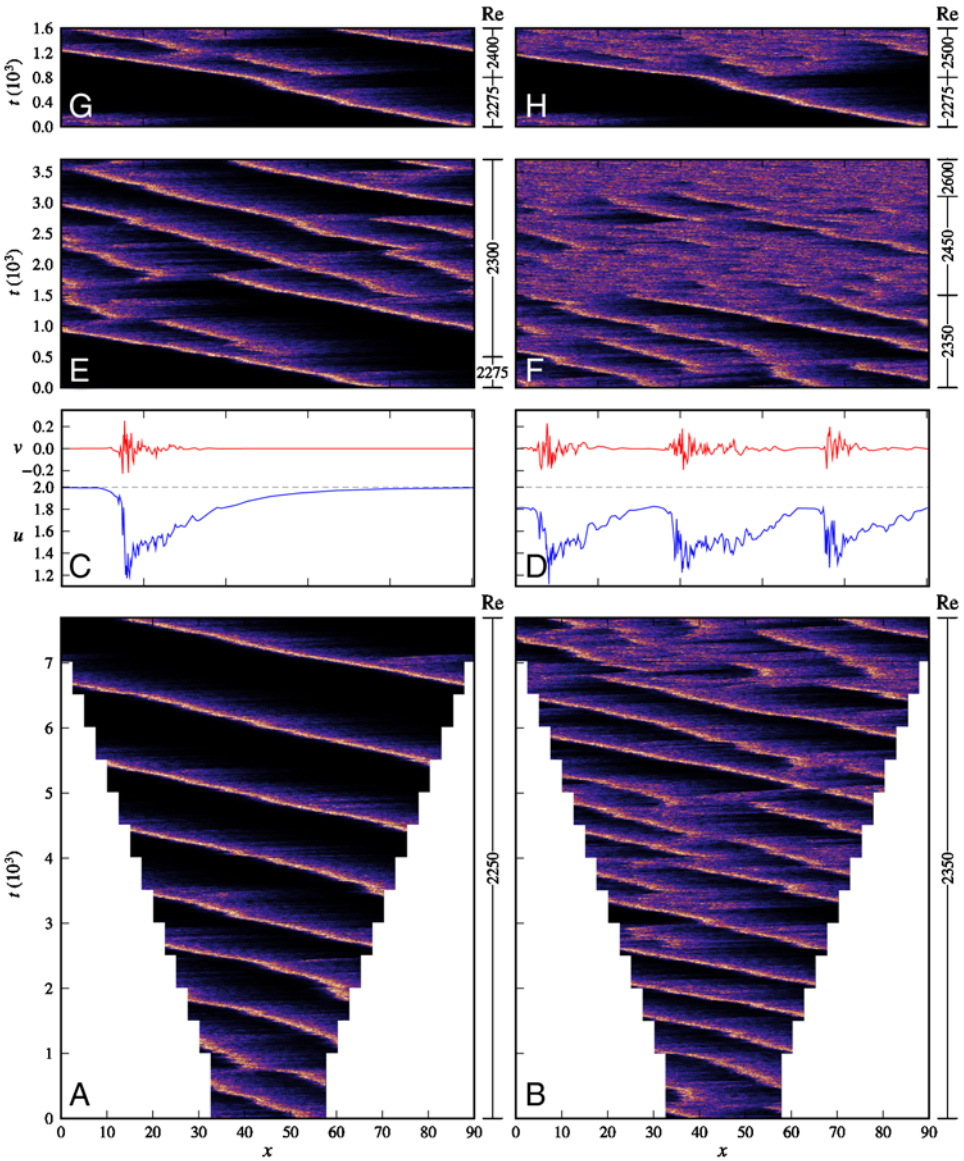

Fig. 2. Simulations highlighting the difference between localized (intensive) turbulence at $\mathrm{Re} = 2{<}250$ (*A*) and (*C*) and extensive, spatio-temporal intermittency at $\mathrm{Re} = 2{<}350$ (*B*) and (*D*). (*A*), (*B*) Space-time diagrams using the same quantity $q(x - \bar{U}t, y = 0, z = 0, t)$ and color scale as in Fig. 1. Simulations are started with a puff in a $L = 25D$ pipe. As time proceeds upwards, L is increased in discrete steps until $L = 90D$. (*C*), (*D*) Streamwise velocity u and one component of transverse velocity v at the final times of (*A*) and (*B*). Laminar parabolic flow along the center line ($u = 2$) is indicated by a dashed line. (*E*) shows a simulation started from a single puff with $\mathrm{Re} = 2,275$, then $\mathrm{Re} = 2,300$, as indicated. (*F*) shows a simulation continuing $\mathrm{Re} = 2,350$ from (*B*) followed by increases to $\mathrm{Re} = 2,450$ and $\mathrm{Re} = 2,600$, as indicated. (*G*), (*H*) Simulations started from a single puff at $\mathrm{Re} = 2,275$ where Re is then increased to 2,400 in (*G*) and 2,500 in (*H*).

at $\mathrm{Re} = 2,250$ an estimate for the characteristic lifetime is over 10^{10} time units (30), astronomically greater than any timescale considered here.

Now consider the case $\mathrm{Re} = 2,350$ shown in Fig. 2*B*. As already noted, as L is increased the number of puffs increases within the pipe so as to maintain approximately the same spatial scale of the turbulent-laminar alternation. The turbulence can be viewed as an extensive quantity—the amount of turbulent flow being dictated by domain size and not by initial conditions. The puffs are less well-defined and between puffs the flow remains separated from parabolic Hagen-Poiseuille flow. Significantly, the turbulent-laminar alternation remains dynamic with intermittent puff splittings and extinctions for as long as we simulate the system. The lower portion of Fig. 2*F* shows a continuation of the simulation $\mathrm{Re} = 2,350$ from Fig. 2*B*.

To better isolate some important characteristics separating the localized and intermittent regimes, and to more accurately determine the critical Re separating the two regimes, we have conducted further simulations shown in Fig. 2 *E*, *G*, and *H*. Simulations are started at $\mathrm{Re} = 2,275$ with a localized puff. In simulations at $\mathrm{Re} = 2,275$ (longer than is shown) the puff remains localized. Fig. 2*E* shows, however, that immediately upon a 1% increase to $\mathrm{Re} = 2,300$, new turbulent patches are initiated downstream from existing ones through puff splitting (28), initially at more-or-less fixed downstream distances and semiregularly in time. Within approximately 1,000 time units, several turbulent patches appear in the $90D$ pipe. Thereafter, turbulent regions interact, and one observes seemingly random, abrupt extinctions of turbulent regions (for example at $t \simeq 1,900$ and $t \simeq 2,800$ in Fig. 2*E*), as well as splitting events. The process gives rise to persistent spatio-temporal intermittency. With available data, we approximate the critical Re for the transition between localized and intermittent behavior as $\mathrm{Re}_1 \simeq 2,300$. This is very close to the value $\mathrm{Re} = 2,320$ where Rotta (31) observes irregular behavior in experiments.

One might expect that the splitting of a turbulent puff would occur more quickly at larger values of Re. However, as seen in Fig. 2*G*, the behavior following an abrupt change to $\mathrm{Re} = 2,400$ is remarkably similar to that at $\mathrm{Re} = 2,300$. At yet higher Re, as in Fig. 2*H*, the spreading is more rapid, but we leave this to other investigations.

Transition Between Intermittent and Uniform Turbulence. As Re increases upward from 2,300 (moving downwards in Fig. 1), intermittent puff splittings and extinctions give rise to an increased proportion of turbulent flow in which puffs are not clearly identifiable. One continues to observe more intense turbulence on the downstream sides of laminar regions much like the trailing edge of a puff. Intermittent events are visually apparent until $\mathrm{Re} = 2,500$, and minor fluctuations can be detected at $\mathrm{Re} = 2,600$, but not at higher Re. Fig. 2*F* shows that this is independent of the direction Re is varied: increasing Re produces a return to uniform turbulence. To study this transition in more detail we have examined three measures as follows.

First we consider the intermittency factor (equivalently the turbulent fraction) γ, since this is the classic measure of the average ratio of turbulent to laminar dynamics within a flow (31). One defines an indicator function $I(x,t)$ to be zero (indicating laminar) or one (indicating turbulence) depending on a threshold for some detector quantity. We again use the transverse velocity magnitude q, for which $q \simeq 0$ for laminar flow. Then

$$I(x,t) = \begin{cases} 1, & q(x,t) > q_*, \\ 0, & \text{otherwise}, \end{cases} \qquad [3]$$

where q_* is a small threshold. Finally, the intermittency factor is defined as $\gamma = \langle I \rangle$, where the average is over all data at each Re.

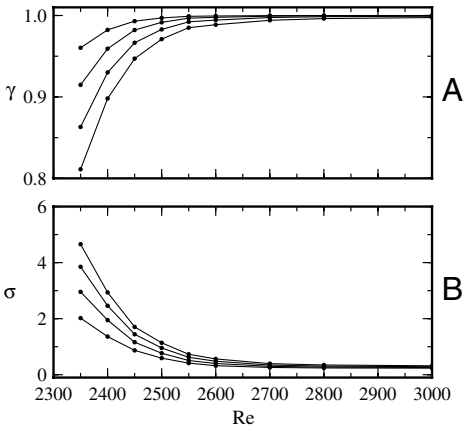

Fig. 3. Transition between intermittency and uniform turbulence. (*A*) Intermittency factor γ as a function of Re for thresholds from $q_* = 4 \times 10^{-3}$ (top curve) to $q_* = 1 \times 10^{-2}$ (bottom curve) in increments of 2×10^{-3}. (*B*) Standard deviation of the size distribution of laminar lengths as a function of Re using the same values of q_* as in (*A*).

Since the indicator, and hence γ, depend explicitly on q_*, it is necessary to vary q_* to properly interpret results.

Fig. 3*A* shows γ for $2,350 \leq \mathrm{Re} \leq 3,000$ at four values of q_*. Whatever the threshold used, the proportion of turbulent flow is seen to increase continuously with Re until $\mathrm{Re} \simeq 2,600$ where it saturates, with $\gamma \simeq 1$.

A second means of quantifying turbulent-laminar dynamics is to directly examine the size distribution of laminar lengths, as has been proposed and studied in a simplified model of plane Couette flow (17). Using the same indicator function, we compute the streamwise length ℓ of each region with $I = 0$ at each time instant. This provides a distribution of laminar lengths from which we compute the standard deviation σ plotted in Fig. 3*B*. Again, whatever the threshold used, there is a continuous decrease in σ with Re until $\mathrm{Re} \simeq 2,600$, followed by Re independence.

Finally, a common statistical measure of a turbulent flow is the single-point probability density function (pdf) of one velocity component. Fig. 4 shows $f(v)$, the normalized pdf of the transverse velocity v, sampled at one point on the pipe axis. It is well-established that f is Gaussian for sufficiently turbulent flow

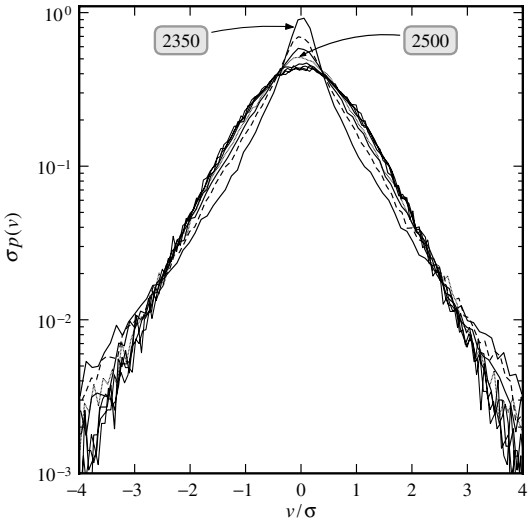

Fig. 4. Normalized, single-point velocity pdfs for $\mathrm{Re} = 2$‹350, 2,400, 2,450, 2,500, 2,600, 2,700, 2,800, and 3,000, as indicated by labels and alternating line types. For $\mathrm{Re} = 2$‹700 and above the distributions are nearly Gaussian. For $\mathrm{Re} = 2$‹600 and below the distributions are non-Gaussian.

(32). This is seen here by the nearly quadratic curves (on a logarithmic scale) for all $\mathrm{Re} \geq 2,700$. As Re is decreased below 2,600 the peaks sharpen and the tails widen. (At $\mathrm{Re} = 2,600$ there is a very small deviation from a normal distribution that is difficult to see in the figure.) The interpretation is that starting at $\mathrm{Re} = 2,600$, the flows possess long-range correlations, different Fourier modes are no longer independent, and velocity distributions are no longer Gaussian. This is consistent with other observations that $\mathrm{Re} = 2,600$ is just at the transition to intermittency.

The three measures just considered show, directly or indirectly, a continuous transition from an intermittent turbulent-laminar state to a state of uniform turbulence at $\mathrm{Re}_2 \simeq 2,600$. For detecting the transition, the velocity pdfs provide the most robust criterion (since no threshold is required) and have the added advantage that they are most easily accessible experimentally.

Stochastic Bifurcation. Following the approach taken in ref. 33, we now consider an analysis of turbulent states that succinctly captures the essence of all three flow regimes and provides a compelling view of the states and their transitions. The length of the pipe L is fixed at $25D$, the approximate length of a single puff. We have simulated 10^4 time units of data for each Re in a range encompassing the transitions. We take the Fourier transform of the transverse velocity magnitude along the pipe axis, $q(x,0,0,t) \to \hat{q}_k(t)$, and focus on $\hat{q}_1$. The modulus of $\hat{q}_1$ is large when the flow possesses a structure on the scale of L, i.e. on the scale of a single puff. The phase of $\hat{q}_1$ merely encodes streamwise position within the periodic pipe. We then view $\hat{q}_1 = re^{i\phi}$ as a complex random variable and for each Re calculate the two-dimensional pdf $\rho(r,\phi)$ by binning the simulation data. Since the streamwise direction is homogeneous, we expect, and the data support, that $\rho(r,\phi)$ is ϕ-invariant. Hence we improve the quality of the estimate of ρ by averaging over ϕ.

Fig. 5 shows ρ for representative Re spanning the range of our study. On the left are gray-scale plots of the pdf in the complex plane. On the right are radial cuts through the pdf: $\rho(r,\phi = 0)$. In order of decreasing Re the following is seen. For $\mathrm{Re} > 2,600$ distributions are almost perfectly Gaussian. Below $\mathrm{Re} = 2,600$ distributions deviate from Gaussian. At $\mathrm{Re} = 2,300$ the peak has clearly moved to finite r. At $\mathrm{Re} = 2,200$ and below the distribution has a single peak at finite r and is zero at $r = 0$.

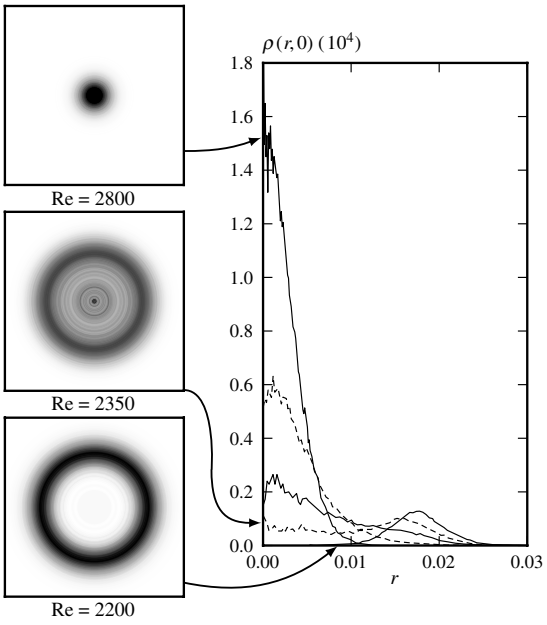

Fig. 5. (*Left*) Contour plots of the two-dimensional axisymmetric pdf $\rho(r,\phi)$ at values of Re indicated, from data in an $L = 25D$ pipe. Black and white correspond to the maximum and minimum of ρ at each Re. (*Right*) Cross-sections of ρ at $\phi = 0$ for Re = 2, 200, 2,300, 2,400, 2,500, and 2,800, as indicated by arrows and alternating line types.

We understand the sequence of states as follows. Above Re_2, turbulence is uniform with Gaussian statistics and the pdf of $\hat{q}_1$ is sharply peaked at zero. The most probable state of the system has no structure on the scale of the $25D$ pipe. This can be viewed as the disordered phase. Below Re_1, turbulence takes the form of equilibrium puffs. The probability of uniform turbulence ($r = 0$) vanishes and the most probable observation is a puff in an arbitrary location in the pipe. This is the ordered phase. Between Re_1 and Re_2 the dynamics are an intermittent mixture of ordered and disordered phases and show a continuous, reversible transition between the two as Re varies.

Discussion

By means of direct numerical simulations in long, periodic pipes we have established transitions between distinct turbulent states in pipe flow near the minimum Re for which turbulence is obtained. We make the following observations about these findings and how they relate to previous and ongoing studies in pipe and other shear flows.

One of the most basic questions one can ask about transition in such flows is, "what is the minimum Reynolds number, Re_c, for which turbulence, once established, will persist?" A fruitful approach has been to find Re_c by examining the decay of relaminarizing turbulent flow and extrapolating decay rates, or inverse lifetimes, to zero (25, 26, 34). However, in 2006, evidence was presented (9), that is now strongly supported by further studies (22, 30), that inverse characteristic lifetimes of reverting turbulence in pipe flow never reach zero at finite Re, suggesting that turbulence is always transient no matter what the value of Re. Significantly, all these measurements are confined to localized puff states.

While it is possible that all turbulence in pipe flow is transient, it does not seem likely. It seems equally unlikely that lifetime measurements of localized puffs will ultimately determine a critical Re. We believe that the key to the transition to sustained turbulence is not in the lifetimes of localized puffs, but in the spatio-temporal aspects of the turbulence investigated here. Pomeau (35) first made the observation that subcritical fluid flows might exhibit a transition to spatio-temporal intermittency similar to that associated with directed percolation (36), a view championed by Manneville for shear-flow transition (17).

Fig. 2 shows that the transition at Re_1 has precisely the qualitative character of a directed-percolation transition and provides evidence directly from a fully resolved numerical simulation that such a transition exists in turbulent flow. Hagen-Poiseuille flow is the absorbing state that once reached is never left (36). Below Re_1 localized regions of turbulence, puffs, do not contaminate neighboring laminar regions (Fig. 2*A*). As suggested by lifetime measurements, these ultimately revert to the absorbing state in finite, but enormously long, time. Above Re_1, however, turbulent regions contaminate downstream laminar flow, as in Fig. 2*E*, *G*, and *H*, and the resulting dynamics is spatio-temporal intermittency. The striking feature of the transition at Re_1 is its abruptness. At $\mathrm{Re} = 2,275$ the contamination probability is zero or very small, while at $\mathrm{Re} = 2,300$ contamination occurs within $O(10^2)$ time units, vastly faster than the characteristic lifetime for decay of a puff. As is well established for directed percolation, once the probability ratio of contamination to decay exceeds a critical value, turbulence has a finite probability of sustaining indefinitely as spatial-temporal intermittency, even though any individual turbulent patch has a finite probability of decay (36). Thus there is a clear mechanism, involving spatio-temporal intermittency, that implicates a change to finite probability of indefinitely sustained turbulence above Re_1.

Irregular turbulent patches within laminar pipe flow have been reported since the original experiments by Reynolds (1) (see

especially ref. 31), and observations of puff splitting near transition go back many years (28). These observations failed to capture the essential point, however, that in a well-defined range $Re_1 \leq Re \leq Re_2$, intermittent turbulent-laminar flows are the intrinsic, asymptotic form of turbulence absent all system noise. Moreover, while near to Re_1 irregularity takes the form of puff splittings and extinctions, intermittent states vary continuously with Re, and nearer to Re_2 intermittency takes the form of laminar flashes in a turbulent background.

Taken in the context of what is known about other shear flows, especially plane Couette flow (12–15, 17), we see a generic and perhaps universal picture emerging for the route from turbulence to laminar flow in subcritical shear flows as Re is reduced to the smallest value that supports turbulence. At Re_2 (whose value depends on the particular flow), uniform turbulence becomes unstable on long length scales and gives rise to an intermittent alternation of turbulent and laminar flow. At some lower value Re_1, this in turn gives rise to localized turbulence within a laminar background and such turbulence has a finite characteristic lifetime. For pipe flow, turbulent-laminar states are never regular except when they are localized. This is contrary to what appear to be robust, steady, delocalized patterns in plane Couette flow (12–14). It is not clear whether or not this distinction is fundamental. The extensive numerical observations presented here, over a range of transition Reynolds numbers, should both motivate experimental studies and serve as a guide to future theory.

ACKNOWLEDGMENTS. We would like to thank M. Avila, C. Connaughton, O. Dauchot, Y. Duguet, B. Hof, R. MacKay, P. Manneville, and A. Willis for helpful discussions. This work was performed using high performance computing resources provided by the University of Warwick Centre for Scientific Computing, funded jointly by the Engineering and Physical Sciences Research Council, and by the Grand Equipement National de Calcul Intensif-Institut du Développement et des Ressources en Informatique Scientifique (Grants 2009-1119 and 2010-1119). D.B. gratefully acknowledges support from the Leverhulme Trust and the Royal Society.

1. Reynolds O (1883) An experimental investigation of the circumstances which determine whether the motion of water shall be direct or sinuous, and of the law of resistance in parallel channels. *Philos T R Soc A* 174:935–982.
2. Eckhardt B, et al. (2009) Theme Issue: Turbulence transition in pipe flow: 125th anniversary of the publication of Reynolds' paper. *Philos T R Soc A* 367:449–599.
3. Darbyshire AG, Mullin T (1995) Transition to turbulence in constant mass flux pipe flow. *J Fluid Mech* 289:83–114.
4. Willis AP, Peixinho J, Kerswell RR, Mullin T (2008) Experimental and theoretical progress in pipe flow transition. *Philos T R Soc A* 366:2671–2684.
5. Mellibovsky F, Meseguer A (2009) Critical threshold in pipe flow transition. *Philos T R Soc A* 367:545–560.
6. Schneider TM, Eckhardt B (2009) Edge states intermediate between laminar and turbulent dynamics in pipe flow. *Philos T R Soc A* 367:577–587.
7. Faisst H, Eckhardt B (2003) Traveling waves in pipe flow. *Phys Rev Lett* 91:224502.
8. Wedin H, Kerswell R (2004) Exact coherent structures in pipe flow: Travelling wave solutions. *J Fluid Mech* 508:333–371.
9. Hof B, Westerweel J, Schneider TM, Eckhardt B (2006) Finite lifetime of turbulence in shear flows. *Nature* 443:59–62.
10. Willis A, Kerswell R (2007) Critical behavior in the relaminarization of localized turbulence in pipe flow. *Phys Rev Lett* 98:014501.
11. De Lozar A, Hof B (2009) An experimental study of the decay of turbulent puffs in pipe flow. *Philos T R Soc A* 367:589–599.
12. Prigent A, Grégoire G, Chaté H, Dauchot O, van Saarloos W (2002) Largescale finite wavelength modulation within turbulent shear flows. *Phys Rev Lett* 89:014501.
13. Prigent A, Grégoire G, Chaté H, Dauchot O (2003) Long wavelength modulation of turbulent shear flows. *Physica D* 174:100–113.
14. Barkley D, Tuckerman LS (2005) Computational study of turbulent laminar patterns in Couette flow. *Phys Rev Lett* 94:014502.
15. Barkley D, Tuckerman LS (2007) Mean flow of turbulent laminar patterns in plane Couette flow. *J Fluid Mech* 576:109–137.
16. Tsukahara T, Seki Y, Kawamura H, Tochio D (2005) DNS of turbulent channel flow at very low Reynolds numbers. *Proceedings of the 4th International Symposium on Turbulence and Shear Flow Phenomena* pp 935–940.
17. Manneville P (2009) Spatiotemporal perspective on the decay of turbulence in wall-bounded flows. *Phys Rev E* 79:025301(R).
18. Blackburn HM, Sherwin SJ (2004) Formulation of a Galerkin spectral element Fourier method for three-dimensional incompressible flows in cylindrical geometries. *J Comput Phys* 197:759–778.
19. McIver DM, Blackburn HM, Nathan GJ (2000) Spectral element Fourier methods applied to simulation of turbulent pipe flow. *ANZIAM J* 42:C954–C977.
20. Chu D, Henderson R, Karniadakis GE (1992) Parallel spectral element Fourier simulation of turbulent flow over riblet mounted surfaces. *Theor Comp Fluid Dyn* 3:219–229.
21. Eggels JGM, et al. (1994) Fully developed turbulent pipe flow: A comparison between direct numerical simulation and experiment. *J Fluid Mech* 268:175–210.
22. Avila M, Willis AP, Hof B (2009) On the transient nature of localized pipe flow turbulence. arXiv:0907.3440v2 [physics.fludyn].
23. Laufer J (1962) Decay of a nonisotropic turbulent field. *Miszellaneen der angewandten Mechanik* 166–174.
24. Badri Narayanan MA (1968) An experimental study of reverse transition in two-dimensional channel flow. *J Fluid Mech* 31:609–623.
25. Narasimha R, Sreenivasan KR (1979) Relaminarization of fluid flows. *Adv Appl Mech* 19:221–309.
26. Peixinho J, Mullin T (2006) Decay of turbulence in pipe flow. *Phys Rev Lett* 96:094501.
27. Wygnanski IJ, Champagne FH (1973) On transition in a pipe. Part 1. The origin of puffs and slugs and the flow in a turbulent slug. *J Fluid Mech* 59:281–335.
28. Wygnanski I, Sokolov M, Friedman D (1975) On transition in a pipe. Part 2. The equilibrium puff. *J Fluid Mech* 69:283–304.
29. Shan H, Ma B, Zhang Z, Nieuwstadt FTM (1999) Direct numerical simulation of a puff and a slug in transitional cylindrical pipe flow. *J Fluid Mech* 387:39–60.
30. Hof B, de Lozar A, Kuik DJ, Westerweel J (2008) Repeller or Attractor? Selecting the dynamical model for the onset of turbulence in pipe flow. *Phys Rev Lett* 101:214501.
31. Rotta J (1956) Experimental contributions to the development of turbulent flow in a pipe. *Ing Arch* 24:258–281.
32. Tavoularis S, Corrsin S (1981) Experiments in nearly homogenous turbulent shear flow with a uniform mean temperature gradient. Part 1. *J Fluid Mech* 104:311–347.
33. Tuckerman LS, Barkley D, Dauchot O (2008) *J Phys Conf Ser* 137:012029.
34. Faisst H, Eckhardt B (2004) Sensitive dependence on initial conditions in transition to turbulence in pipe flow. *J Fluid Mech* 504:343–352.
35. Pomeau Y (1986) Front motion, metastability and subcritical bifurcations in hydrodynamics. *Physica D* 23:3–11.
36. Henkel M, Hinrichsen H, Lübeck S (2009) *Non-equilibrium Phase Transitions* (Springer, New York), 1st ed.